Citation: BoneKEy Reports **3**, Article number: 543 (2014) | doi:10.1038/bonekey.2014.38

www.nature.com/bonekey

ORIGINAL ARTICLE

Functional heterogeneity of osteocytes in FGF23 production: the possible involvement of DMP1 as a direct negative regulator

Ji-Won Lee[1,2], Akira Yamaguchi[2] and Tadahiro Iimura[1,2,3]

[1]Division of Bio-Imaging, Proteo-Science Center (PROS), Ehime University, Ehime, Japan. [2]Department of Oral Pathology, Graduate School of Medical and Dental Sciences, Tokyo Medical and Dental University, Tokyo, Japan. [3]Translational Research Center and Artificial Joint Integrated Center, Ehime University Hospital, Ehime, Japan.

Fibroblast growth factor 23 (FGF23) and dentin matrix protein (DMP1) are hallmarks of osteocytes in bone. However, the mechanisms underlying the actions of DMP1 as a local factor regulating FGF23 and bone mineralization are not well understood. We first observed spatially distinct distributions of FGF23- and DMP1-positive osteocytic lacunae in rat femurs using immunohistochemistry. Three-dimensional immunofluorescence morphometry further demonstrated that the distribution and relative expression levels of these two proteins exhibited reciprocally reversed patterns especially in midshaft cortical bone. These *in vivo* findings suggest a direct role of DMP1 in FGF23 expression in osteocytes. We next observed that the inoculation of recombinant DMP1 in UMR-106 osteoblast/osteocyte-like cells and long-cultured MC3T3-E1 osteoblastic cells showed significant downregulation of FGF23 production. This effect was rescued by incubation with an focal adhesion kinase (FAK) inhibitor or MEK (mitogen-activated protein kinase (MAPK)/extracellular signal regulated kinase (ERK)) inhibitor but not inhibitors of phosphoinositide 3-kinase or Rho kinase. Consistently, the levels of phosphorylated FAK, ERK and p38 were significantly elevated, indicating that exogenous DMP1 is capable of activating FAK-mediated MAPK signaling. These findings suggest that DMP1 is a local, direct and negative regulator of FGF23 production in osteocytes involved in the FAK-mediated MAPK pathway, proposing a relevant pathway that coordinates the extracellular environment of osteocytic lacunae and bone metabolism.

BoneKEy Reports **3**, Article number: 543 (2014) | doi:10.1038/bonekey.2014.38

Introduction

Osteocytes are cells embedded in the lacunae of the hard bone tissue that extend their cellular processes in narrow bony tunnels of the canaliculi, establishing an osteocytic lacuno-canalicular network that runs throughout the bone matrix.[1–3] This network guarantees the supply of nutrition to distant osteocytes and allows the transit of small molecules and minerals that originate from the extracellular fluid. Furthermore, it enables direct intercellular communication among osteocytes, thus establishing an osteocyte network. The canaliculi and osteocytic cellular processes often reach the bone surface, through which osteocytes directly interact with other types of bone cells, osteoblasts and osteoclasts. Osteocytes account for 90–95% of all bone cells, with the remainder of cells being osteoblasts and osteoclasts. With regard to the unique architecture and composition of bone cells, evidence has emerged in recent years that has significantly changed the conventional view of osteocytes as passive placeholders in bone to pivotal and versatile orchestrators of bone remodeling and mineralization. As a major function, osteocytes are thought to respond to mechanical strain and accordingly exert biochemical signals that regulate the activities of osteoblasts and osteoclasts.[4–9] Osteocytes also function as endocrine cells by producing fibroblast growth factor 23 (FGF23), which regulates calcium and phosphate homeostasis targeting tissues other than bone, such as the kidneys.[3,10,11]

FGF23 was originally identified in the ventrolateral thalamic nucleus of the brain.[12] Although FGF23 mRNA is found in several tissues, this molecule is most abundantly expressed in bone, predominantly in osteocytes.[13–18] FGF23 essentially

Correspondence: Professor A Yamaguchi, Department of Oral Pathology, Graduate School of Medical and Dental Sciences, Tokyo Medical and Dental University, 1-5-45 Yushima, Tokyo 113-8549, Japan.
E-mail: akira.mpa@tmd.ac.jp or Dr T Iimura, Division of Bio-Imaging, Proteo-Science Center (PROS), Ehime University, Ehime 791-0295, Japan.
E-mail: iimura@m.ehime-u.ac.jp

Received 29 September 2013; accepted 11 February 2014; published online 4 June 2014

downregulates the serum levels of phosphate by inhibiting the absorption and reabsorption of phosphate from the gut and kidneys, respectively. In the kidneys, this hormone reduces the expression of sodium–phosphate transporters (type IIa and IIc) in the renal proximal tubular membrane, thereby downregulating phosphate reabsorption, thus resulting in the excretion of phosphate.[19,20] FGF23 reduces the 1,25-dihydroxyvitamin level by inhibiting the renal 1-α-hydroxylase expression and promoting the 24-hydroxylase expression, thereby downregulating the amount of phosphate absorption from the gut and resorption from the bone.[21,22] Mutual regulation of FGF23 and parathyroid hormone has been reported in rodent models[23,24] and identified in clinical cases of hypophosphatemic rickets and chronic kidney disease.[25]

In addition to these systemic and hormonal patterns of regulation, the FGF23 expression appears to be regulated locally by FGF23-producing cells and osteocytes through molecules such as dentin matrix protein-1 (DMP1)[26,27] and the phosphate-regulating gene with homology to endopeptidases on X chromosome (PHEX),[28] both of which are highly expressed in osteocytes. DMP1 is a member of the small integrin-binding ligand *N*-linked glycoprotein family of extracellular non-collagenous matrix proteins present in the mineralized matrix of dentin and bone.[29–32] DMP1 has a high negative charge, and similar to other family members it has been postulated to have an important role in mineralized tissue formation, more specifically, via the initiation of nucleation and the modulation of mineral phase morphology. *Dmp1*-deficient mice exhibit osteomalacia and rickets owing to elevated FGF23 levels in osteocytes. PHEX is a metalloendopeptidase and, although its biochemical function remains to be fully elucidated, it has an important role in phosphate homeostasis, as mice carrying the *Phex* mutation have a similar phenotype to *Dmp1* deficiency.[26,28] Although these genetic findings solidify the idea that DMP1 and PHEX are local negative regulators of FGF23 production in osteocytes, how these molecules regulate FGF23 has yet to be thoroughly described.

This study focused on the functional role of DMP1 in FGF23 production by using approaches of immunofluorescence morphometry[33–35] and *in vitro* cell culture systems. Our *in vitro* observations and results of *in vivo* analyses suggest a functional role of DMP1 as a local and direct regulator of FGF23 production in osteocytes.

Results and Discussion

Distinct expression and distribution patterns of FGF23 and DMP1 proteins in the osteocytic lacunae of cortical bone

To understand whether osteocytes compose functionally homogeneous or heterogeneous populations in their specific protein production, we first investigated the distribution patterns of FGF23- and DMP1-positive osteocytic lacunae and Sclerostin- and DMP1-positive osteocytic lacunae in distinct portions of 16-week-old femurs by means of double immunofluorescence using two combinations of antibodies against FGF23/DMP1 and Sclerostin/DMP1 (**Figure 1a**). In the trabecular portion of metaphysis, FGF23-positive lacunae were scarcely detectable, whereas most of the lacunae were

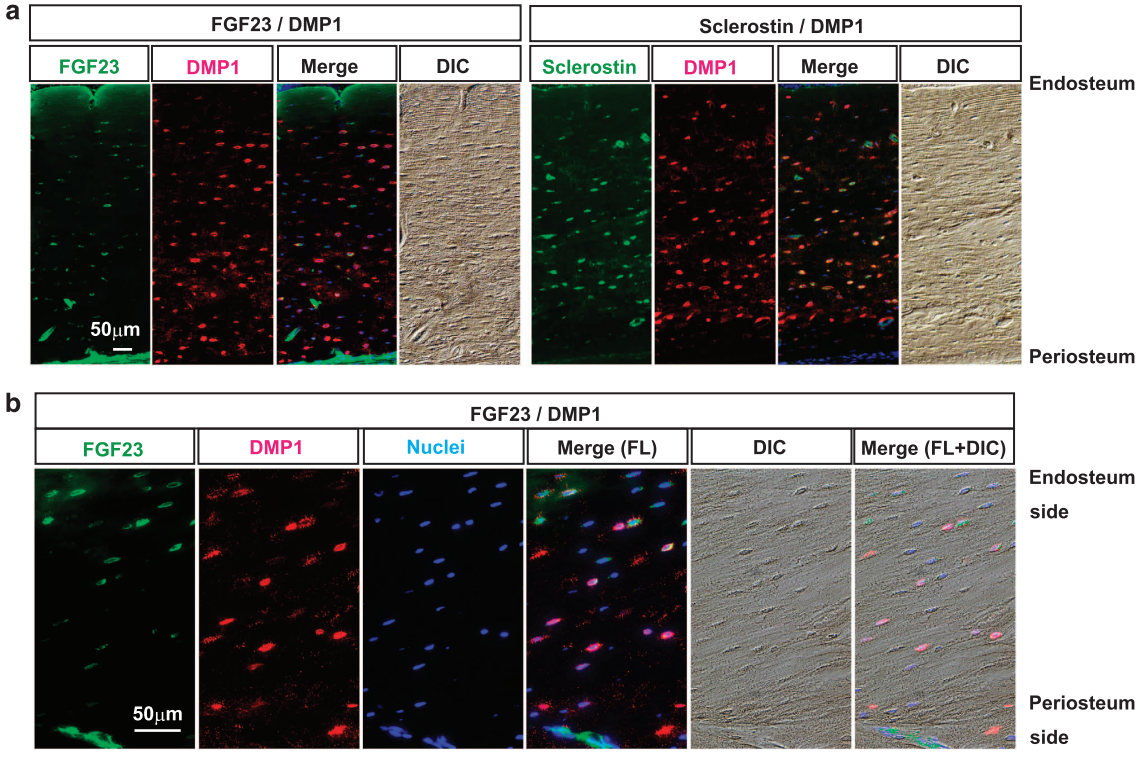

Figure 1 Distinct localization of FGF23 and DMP1 in cortical osteocytes. (**a**) Double immunofluorescence stainings for FGF23/DMP1 and sclerostin/DMP1 were performed with femur sections obtained from 16-week-old rats. FGF23 and DMP1 were detected by secondary antibodies conjugated with Alexa Fluor 488 (in green) and 568 (in red), respectively. The sections were counterstained with 4′-6-diamidino-2-phenylindole to detect nuclei (in blue). Differential interference contrast (DIC) images of each section were obtained for morphological observation. Merged images are shown in the right panels. Scale bar: 50 μm. Endosteal side is up. (**b**) Magnified images of double immunofluorescence stainings for FGF23/DMP1 of another specimen from a 16-week-old rat. Scale bar: 50 μm. Endosteal side is up. FL; fluorescence.

DMP1-positve (data not shown), as previously described.[18] However, much larger numbers of FGF23-positive lacunae were observed in the cortical bone of the diaphysis, whereas DMP1 signals were detectable in most of the lacunae, as was observed in the trabecular bone (**Figure 1a**). Notably, most of the FGF23-positive lacunae in this bone site tended to be predominantly located in the endosteal portion, not in the periosteal portion, thereby demarcating FGF23-positive and FGF23-negative areas in cortical bone, although DMP1-positive lacunae were detectable in the entire areas (**Figure 1a**, left panels). In contrast to this observation, larger numbers of Sclerostin-positive lacunae compared with FGF23-postive lacunae were detectable, and most of the Sclerostin-positive lacunae were overlapped with DMP1-positive lacunae, which were recognized by yellow or orange signals in a merged picture of green and red fluorescence colors (**Figure 1a**, right panels).

These distinct distribution patterns of FGF23- and DMP1-positive lacunae in cortical bone were confirmed by magnified views of double immunofluorescence using antibodies against FGF23 and DMP1, which demonstrated distinct distribution patterns of FGF23- and DMP1-positive lacunae, categorized into three populations: FGF23(+)/DMP1(−), FGF23(+)/DMP1(+) and FGF23(−)/DMP1(+) (**Figure 1b**).

To further confirm this observation in a quantitative manner, we took advantage of three-dimensional double immunofluorescence morphometry.[33–35] Confocal microscopy-based optical slices were three-dimensionally reconstructed *in silico*, and the relative fluorescence intensity of the FGF23 and DMP1 signals in the lacunae in the same optical sections was measured by focusing on the midshaft region of a 16-week-old femur as a representative bone site (**Figure 2**). This analysis allowed us to observe the spatial distribution of these proteins in bone tissue and each single lacuna (shown in green and red for FG23 and DMP1, respectively, in **Figure 2a**, surface) with their relative expression levels (shown in graded colors in **Figure 2a**, gradient). Interestingly, the statistical analysis based on this imaging method demonstrated that the DMP1 expression level in each lacuna was significantly higher in the periosteum than in the endosteum region, whereas the level of FGF23 showed the reverse pattern (**Figure 2b**). These analyses indicate that the distribution and expression levels of FGF23 and DMP1 in osteocytic lacunae exhibit reciprocally reversed patterns, especially in midshaft cortical bone. We also noticed that there is a trend that high levels of FGF23 were detectable by osteocytic lacunae that were longitudinally well arranged along lamellar structure of the bone and encase smaller levels of extracellular DMP1. As DMP1-null mice demonstrate augmented levels of FGF23, it is well accepted that DMP1 is genetically a negative regulator of the FGF23 production.[26] Therefore, our detailed *in vivo* observations raise the possibility that extracellular DMP1 may negatively regulate FGF23 production in osteocytes.

Exogenous DMP1 downregulates FGF23 expression and production

To investigate the possible role of DMP1 in FGF23 regulation, we first assessed whether exogenous DMP1 regulates the levels of *fgf23* gene expression and FGF23 production using

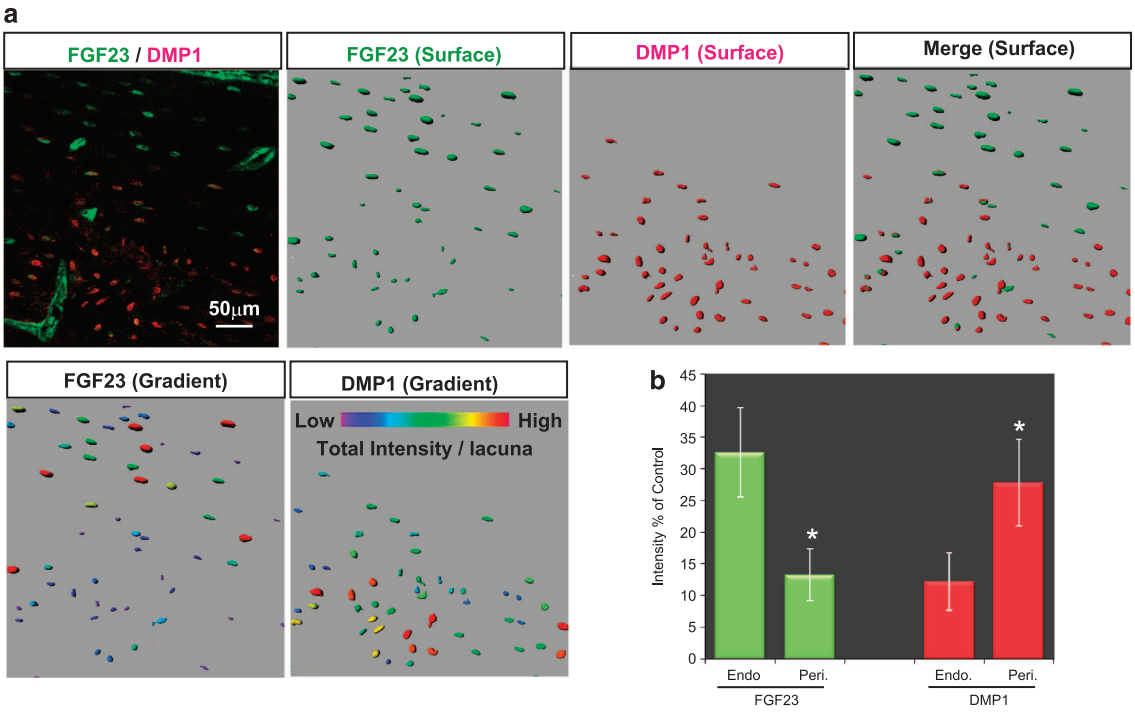

Figure 2 Distinct spatial distributions and relative expression levels of FGF23 and DMP1 on three-dimensional (3D) immunofluorescence morphometry. (**a**) Representative confocal 3D-reconstituted images of the confocal z-series slices stained with double immunofluorescence FGF23 (in green) and DMP1 (in red) obtained from the femurs of 16-week-old rats. Scale bar: 50 μm. Easy 3D fluorescence image (upper left), surface rendering images of FGF23 (in green), DMP1 (in red) and their merged image are shown. The relative expression levels of FGF23 and DMP1 are demonstrated by graded colors (lower panels). Scale bar: 50 μm. Endosteal side is up. (**b**) The relative fluorescence intensity of FGF23 and DMP1 in the endosteal (Endo) portion and periosteal (Peri) portion was statistically compared. *endosteal vs periosteal, $P<0.05$. The data are representative of at least three independent experiments.

UMR-106 osteoblastic cells. Rat UMR-106 is a well-characterized osteoblastic cell model[36–39] that exhibits a tendency to express FGF23, as well as osteoblastic phenotypes.[40–43] Therefore, UMR-106 cells are thought to possess surrogate characteristics of the osteoblast/osteocyte lineage. The cells were treated with 10, 50 and 100 ng ml^{-1} recombinant DMP1 for 24 h. As shown in **Figure 3a**, DMP1 significantly reduced the gene expression of *fgf23*. In addition, the production of FGF23 proteins in the conditioned medium was also markedly inhibited dose dependently by treatment with DMP1, as tested by ELISA (**Figure 3b**). Treatment with other arginine–glycine–aspartate (RGD)-containing proteins such as osteopontin, human and mouse matrix extracellular phosphoglycoprotein also tended to decrease the FGF23 production, especially at their higher doses (500 ng ml^{-1}); therefore, DMP1 most effectively downregulated FGF23 production (**Figure 3b**). DMP1 treatment did not cause significant changes in cell number (**Figure 3c**); therefore, it is likely that the downregulation of the FGF23 production induced by exogenous DMP1 was a direct effect.

Exogenous DMP1 augments the formation of focal adhesions

As it has been established that DMP1 triggers the formation of focal adhesion points through the actions of the cell surface receptor, αVβ5 integrin,[44,45] we next assayed the effects of exogenous DMP1 on the formation of focal adhesion and cellular morphology using immunohistochemical staining for anti-vinculin in two osteoblastic cell lines: UMR-106 and MC3T3-E1 (**Figures 3c and d**). The cells were counterstained with fluorescent dye-conjugated phalloidin and scanned using high-resolution optical slices of the confocal *z*-series. Three-dimensional morphometry was conducted to measure morphological changes and count the number of points of focal adhesion. The number of focal adhesion points, cell surface volume and surface area was significantly increased with DMP1 treatment in both cell lines (**Figure 3d**).

We further tested whether this DMP1 treatment (100 ng ml^{-1}) of UMR-106 cells regulates other osteoblastic and osteocytic markers by quantitative real-time PCR (**Figure 4a**). As results, *col1a1*, *Runx2* and *SOST/Sclerostin* were significantly downregulated, whereas *DMP1* expression level was significantly upregulated by exogenous DMP1. These data indicate that exogenous DMP1 treatment was sufficient to trigger the formation of areas of focal adhesion in these osteoblastic cells, concomitant with the downregulation of FGF23 production and the changes in other marker expression levels (**Figures 3** and **4a**).

The regulation of FGF23 production by DMP1 is mediated by the focal adhesion kinase (FAK)- mitogen-activated protein kinase (MAPK) axis

We further investigated intracellular pathways that regulate FGF23 via the actions of DMP1 (**Figures 4b–d**). It is well established that cell surface integrins mediate intracellular signals that orchestrate many aspects of cell behavior, including proliferation, survival, shape, polarity, motility and gene

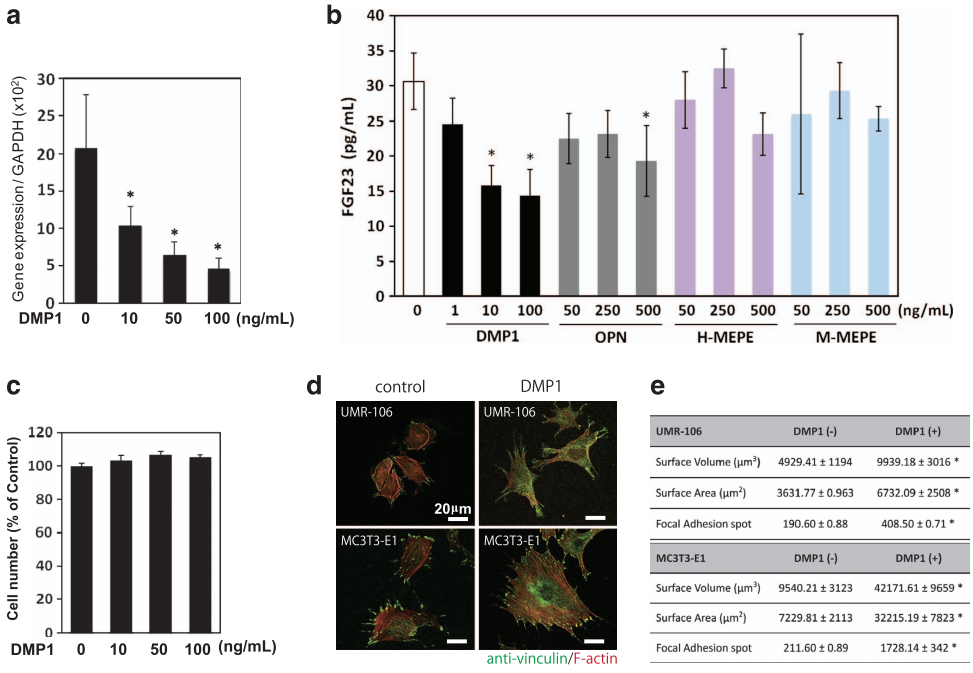

UMR-106	DMP1 (-)	DMP1 (+)
Surface Volume (μm^3)	4929.41 ± 1194	9939.18 ± 3016 *
Surface Area (μm^2)	3631.77 ± 0.963	6732.09 ± 2508 *
Focal Adhesion spot	190.60 ± 0.88	408.50 ± 0.71 *
MC3T3-E1	**DMP1 (-)**	**DMP1 (+)**
Surface Volume (μm^3)	9540.21 ± 3123	42171.61 ± 9659 *
Surface Area (μm^2)	7229.81 ± 2113	32215.19 ± 7823 *
Focal Adhesion spot	211.60 ± 0.89	1728.14 ± 342 *

Figure 3 Downregulation of the fgf23 expression and its protein production by exogenous DMP1. (**a**, **b**) UMR-106 cells were cultured with recombinant DMP1 at a concentration of 10, 50 and 100 ng ml^{-1}, and with other RGD-containing proteins, osteopontin, human matrix extracellular phosphoglycoprotein (H-MEPE) and mouse MEPE (M-MEPE) at indicated concentrations. After 24 h, total RNA was extracted from the cells, and the expression levels of *fgf23* were analyzed using quantitative real-time PCR. The secreted protein levels of FGF23 in the cell culture supernatant were determined using ELISA. *$P<0.05$. The data are representative of at least three independent experiments. (**c**) Effect of the DMP1 treatment on the number of cells was assayed by (3-(4,5,dimethylthiazol-2-yl)-2,5-diphenyltetrazolium bromide) (MTT)-based assay. Effects of exogenous DMP1 on focal adhesion formation and cellular morphology (**d**, **e**) UMR106 and MC3T3-E1 cells were treated with or without DMP1 (100 ng ml^{-1}). After 24 h, the cells were fixed and subjected to immunocytochemistry. (**d**) Anti-vinculin (in green) was used to observe the presence of focal adhesion, and F-actin was stained with tetramethylrhodamine (TRITC)-conjugated phalloidin (in red). (**e**) The number of focal adhesion points and the cellular volume and surface area were statistically analyzed on the three-dimensional-reconstituted images. *$P<0.05$. The data are representative of at least three independent experiments. RGD, arginine–glycine–aspartate.

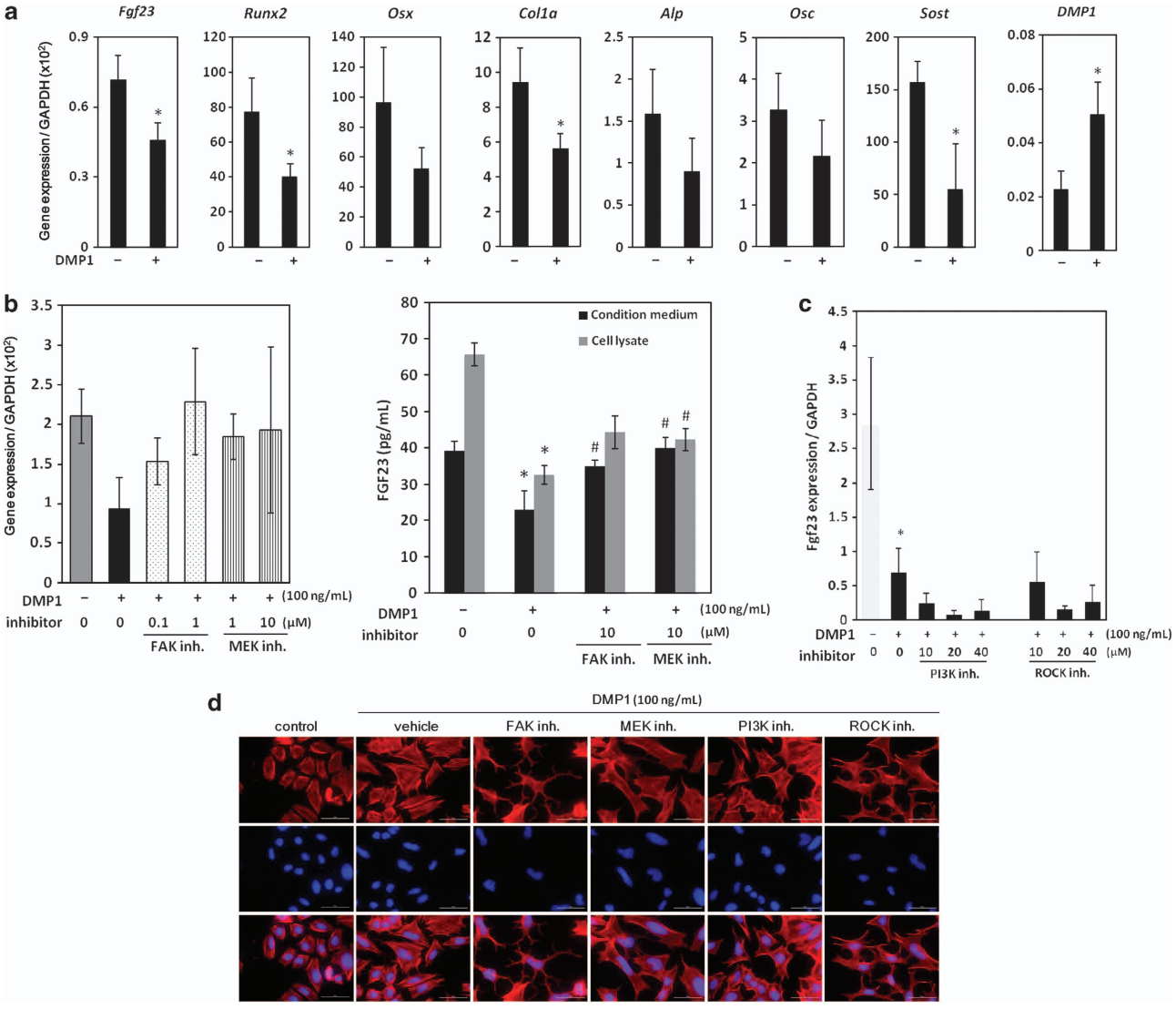

Figure 4 Effects on expression levels of osteoblastic and osteocytic markers and involvement of the FAK-mediated MAPK pathway in the regulation of FGF23 by exogenous DMP1. (**a**) Expression levels of *Fgf23, Runx2, Osterix, Col1a1*, bone-type alikaline phosphatases (*Alp*), Osteocalcin (*Osc*), *Dmp1* and *SOST* in the presence (100 ng ml^{-1}) and absence of DMP1 were compared. (**b**) UMR-106 cells were treated with FAK or MEK inhibitor (inh.) in the presence of DMP1 (100 ng ml^{-1}). After 24 h, total RNA was collected from the cells, and the expression levels of *fgf23* were analyzed using quantitative real-time PCR. Protein levels of FGF23 in the cell culture supernatant and cell lysate were determined using ELISA. *Control vs DMP1; #DMP1 vs inh., $P<0.05$. (**c**) Cells were cultured with or without the PI3K or ROCK inh. in the presence of DMP1 (100 ng ml^{-1}). After 24 h, total RNA was extracted from the cells, and the expression levels of *fgf23* were analyzed using quantitative real-time PCR. *Control vs DMP1, $P<0.05$. (**d**) After 24 h of treatment under the same conditions, cells were incubated in Alexa Fluor 568-conjugated phalloidin (red) and 4′-6-diamidino-2-phenylindole (blue) for actin and nuclei, respectively. Merged images are shown in the lowest panels. The data are representative of at least three independent experiments. MEK, MAPK/extracellular signal related kinase; GAPDH, glyceraldehyde 3-phosphate dehydrogenase.

expression and differentiation, which include the pathways of FAK, MAPK, phosphoinositide 3-kinase (PI3K) and Rho kinase (ROCK).[46] Four distinct inhibitors were added to UMR-106 cells in the presence of exogenous DMP1. As observed in **Figure 3**, the mRNA expression of *fgf23* was significantly decreased by DMP1 treatment (**Figure 4b**). However, these effects were markedly rescued by adding either the FAK inhibitor or the mitogen-activated protein kinase inhibitor. Consistently, protein production levels in cells and conditioned media were downregulated by DMP1 treatment, and this effect was significantly recovered by either of these inhibitors, thus suggesting that FGF23 production is affected by DMP1 stimulation through the FAK-MAPK axis. We next investigated whether signal pathways other than the MAPK pathway are involved in the regulation of FGF23 production in UMR-106 cells by treating cells with inhibitors of PI3K and ROCK (**Figure 4c**). The downregulated FGF23 expression induced by DMP1 was not recovered by adding either the PI3K inhibitor or ROCK inhibitor at any dose.

We further observed changes in cellular morphology by these inhibitor treatments by using cellular actin staining by fluorescence-labeled phalloidin (**Figure 4c**). Interestingly, the morphological changes caused by exogenous DMP1 were perturbed by the FAK or ROCK inhibitor but not by the inhibitors of mitogen-activated protein kinase or PI3K, suggesting that the cellular morphological changes induced by DMP1 are likely mediated by the FAK-ROCK pathway in osteoblastic cells. Taken together, the results suggest that the downregulation of

FGF23 production by DMP1 is specifically mediated by the FAK-MAPK axis (**Figure 4d**).

To further investigate the effects of DMP1 on FGF23 expression and production in osteocytic cells, we took advantage of long-cultured osteoblastic cells. MC3T3-E1 cells regularly do not express an osteocytic phenotype; however, long culture under osteogenic differentiation medium reportedly allows these cells to produce an osteocytic phenotype, such as that involving the DMP1 or FGF23 production (**Figure 5a**).[47] Treatment of the long-cultured MC3T3-E1 cells with DMP1 (100 ng ml^{-1}) significantly downregulated *fgf23* expression, whereas endogenous *Dmp1* expression level was significantly upregulated (**Figure 5b**). These findings were consistent with the observations in UMR106 cells, although other markers that we investigated did not show significant changes in the long-cultured MC3T3-E1 cells (**Figure 5b**).

We next investigated the signaling pathways in the long-cultured MC3T3-E1 cells. Exogenous DMP1 dose dependently suppressed the *fgf23* expression and its protein production, as observed in the UMR-106 cells (**Figures 6a and b**). This downregulation effect was partially but significantly recovered by both the FAK and MAPK inhibitors. To biochemically confirm the activation of the FAK-MAPK signaling pathway by DMP1 treatment in the long-cultured MC3T3-E1 cells, the cells were treated in the absence or presence of the FAK inhibitor for 24 h, and whole proteins were collected for a western blot analysis. As shown in **Figure 6c**, the levels of phosphorylated FAK, extracellular signal regulated kinase (ERK) and p38 were obviously elevated, indicating that the DMP1 treatment activated FAK-MAPK signaling. To confirm that the observed activation was specific, we tested the effects of the FAK inhibitor on the observed response to DMP1. The mitogen-activated protein kinase activity is required for the phosphorylation of ERK1/2 and subsequent ERK-mediated signal transduction. Indeed, when DMP1 (100 ng ml^{-1})-treated cells were treated with 1 and 10 μM of the FAK inhibitor for 24 h, the phosphorylation levels of FAK, ERK and p38 were significantly reduced, indicating that DMP1 activated MAPK signaling through the activation of FAK in the long-cultured MC3T3-E1 cells.

The results of the *in vivo* and *in vitro* analyses described above strongly suggest that DMP1 is a local and direct regulator of the FGF23 production in osteocytes, largely through its actions in the FAK-mediated MAPK pathway. Several possible mechanisms underlying the regulation of FGF23 production in osteocytes by DMP1 have been proposed.[48] As DMP1 proteins have been demonstrated to be localized in cell nuclei, it has been proposed that DMP1 participates in transcriptional regulation.[49] Our observations do not support this phenomenon in terms of FGF23 expression. The other model suggests that DMP1 negatively regulates an unknown, local, bone-derived 'FGF23-stimulating factor.' The findings observed in this report do not exclude this possibility, but rather propose a more direct effect of DMP1 on FGF23 regulation in osteocytes, possibly via the MAPK pathway.

The extracellular environment in the osteocytic lacunar canalicular system bridges local FGF23 regulation and bone metabolism

Feng *et al.*[26] reported that DMP1-null mice exhibit augmented levels of FGF23 and a striking lack of osteocyte processes in which osteocytes do not appear to be able to attach to their lacunae. Our *in vitro* observations in this study are consistent with the findings of this previous report and further suggest that FAK-mediated signaling has a pivotal role in the maintenance of the proper shape of osteocytes and their network, concomitant with the regulation of *FGF23* expression mediated by the MAPK pathway. Therefore, DMP1 bridges the structural properties and functional characteristics of osteocytes by stimulating multiple

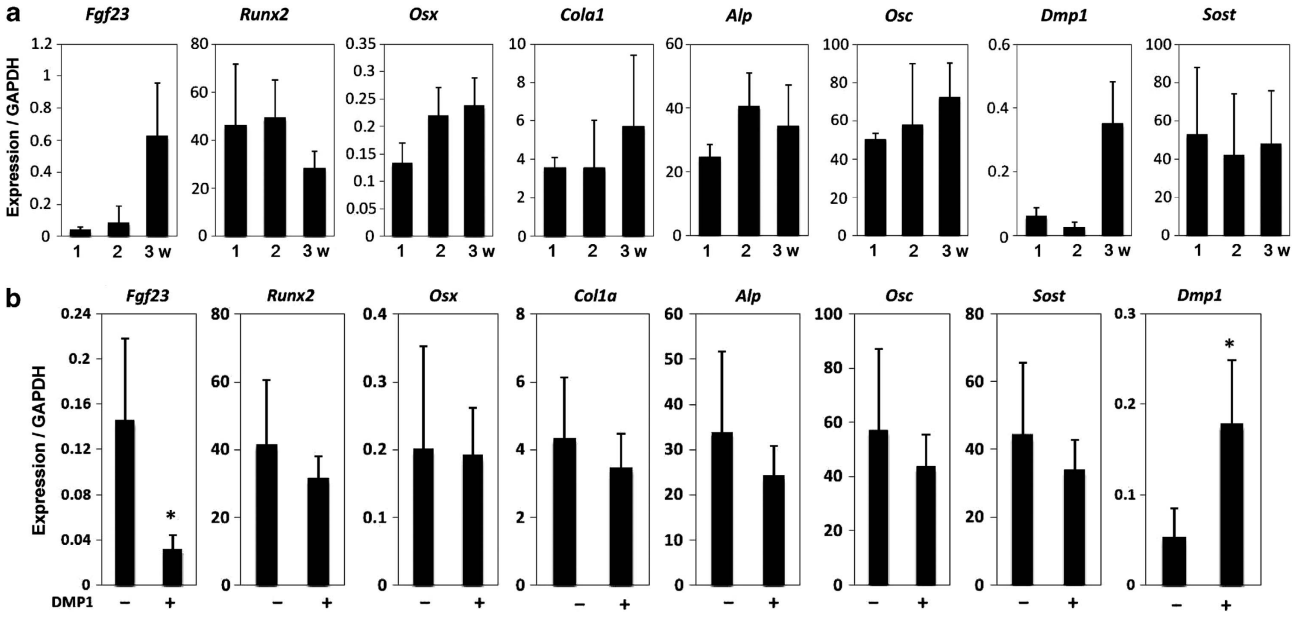

Figure 5 Temporal expression patterns of osteoblastic and osteocytic markers in the long-cultured osteoblastic MC3T3-E1 cells, and the effects of DMP1 treatment on these markers. (**a**) After 1, 2 and 3 weeks of culture of MC3T3-E1 cells in osteogenic medium, expression levels of *Fgf23, Runx2, Osterix, Col1a1*, bone-type alkaline phosphatases (*Alp*), Osteocalcin (*Osc*), *Dmp1 and SOST* s were analyzed by quantitative real-time PCR. (**b**) After 4 weeks of culture with or without DMP1, the gene expression levels were compared. GAPDH, glyceraldehyde 3-phosphate dehydrogenase.

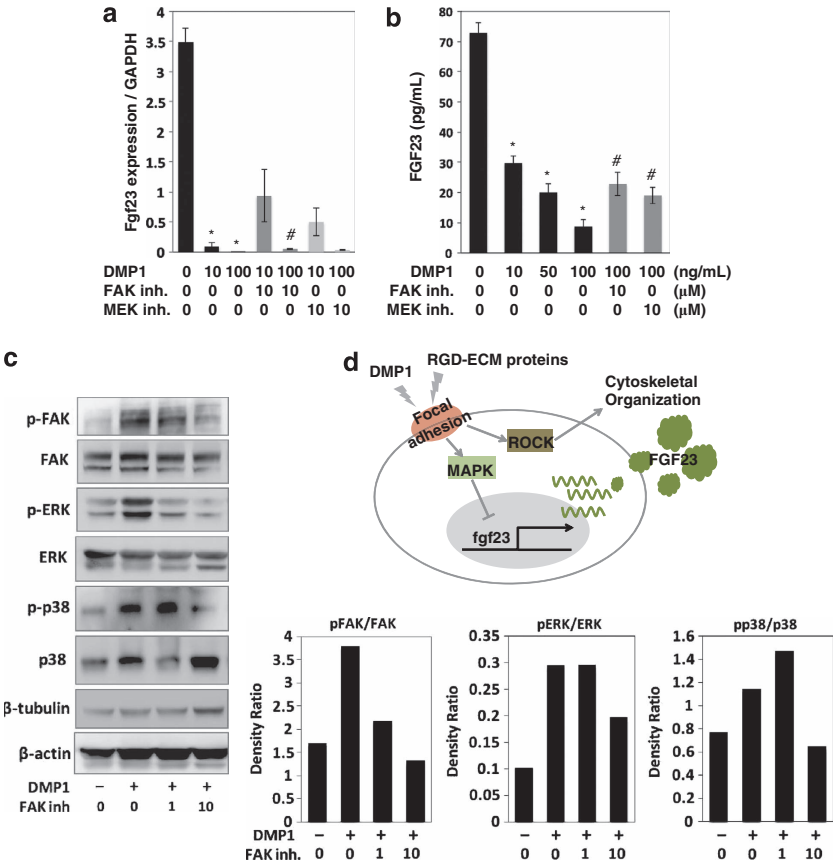

Figure 6 Effects of DMP1 on the FGF23 production and MAPK signaling in the long-cultured osteoblast cells. (**a**) Cells were cultured with DMP1 at a concentration of 10 and 100 ng ml $^{-1}$. After 24 h, total RNA was extracted from the cells, and the expression levels of *fgf23* were analyzed using quantitative real-time PCR. (**b**) The secreted protein levels of FGF23 in the cell culture supernatant were determined using ELISA. *Control vs DMP1; $^{\#}$DMP1 vs Inhibitor (inh.), $P<0.05$. (**c**) Cells were treated with the FAK inh. in the presence of DMP1. After 24 h, the cell lysates were collected and separated using 10% SDS-polyacrylamide gel electrophoresis. The levels of phosphorylated and non-phosphorylated FAK, ERK and p38 were determined using western blotting. The level of β-tubulin and β-actin were evaluated as an internal control. The data are representative of at least three independent experiments. (**d**) A possible model for the local regulation of the FGF23 expression by DMP1 and other RGD-containing exracellular matrix (ECM) proteins. Stimulation of DMP1 and RGD-containing ECM proteins to induce focal adhesion formation regulates a broad range of key cellular signals, such as those involved in the MAPK and ROCK pathways. As a result of stimulation with DMP1 and other RGD-containing ECM proteins, the FGF23 expression was downregulated by the MAPK pathway, but not the PI3K or ROCK pathway. In addition, the ROCK pathway is involved in cytoskeletal reorganization. ERK, extracellular signal regulated kinase; RGD, arginine–glycine–aspartate.

focal adhesion-mediated intercellular signals. In support of this concept, Kamioka *et al.*[50] reported that molecules associated with focal adhesion are predominantly found in osteocytic cellular processes but not in cell bodies. Our *in vitro* findings also suggest that DMP1 is not the only molecule to be involved in the regulation of cellular shape and FGF23 production; other RGD-containing extracellular molecules may be involved. Therefore, it is likely that the extracellular environment in each osteocytic lacuna contributes to the regulation of FGF23 (**Figure 6d**). Nevertheless, our data indicate that DMP1 exhibits the downregulation effect on FGF23 production most effectively among RGD-containing proteins possibly through enhancing the expression level of *Dmp1* itself (**Figures 4a** and **5a**).

Along this line, the regulatory production of FGF23 in osteocytes is tightly associated with bone formation and maturation. On the basis of a series of immunohistochemistry studies, Ubaidas *et al.*[18] proposed that the primary source of FGF23 is osteocytes established after physiological bone remodeling. This interpretation is consistent with our observations in the sense that hypermineralized mature lacunae possibly decrease their amount of DMP1 and become prone to enhancing the *fgf23* expression in their encased osteocytes. Consistent with these findings, Samadfam *et al.* demonstrated that the regulation of FGF23 production depends on the prevailing turnover rate of bone.[41] For example, exogenous parathyroid hormone[1–34] administration in wild-type mice increases bone turnover and elevates the expression of *DMP1* in bone tissue, whereas the gene expression of *fgf23* is reduced, suggesting that DMP1 is a key regulator of FGF23 related to bone turnover. This may also explain the fact that a significantly lower number of osteocytes exhibit detectable levels of the FGF23 protein expression compared with that noted in trabecular bone, likely owing to the distinct bone turnover rate observed in these bone sites.[18]

FGF23 production was mostly detectable in longitudinally arranged and spindle-shaped lacunae in lamellar bone (**Figure 2**). The formation of longitudinally arranged and spindle-shaped osteocytes is highly associated with mechanical loading during postnatal bone development.[35,51] Therefore, functional heterogeneity of osteocytes in FGF23 production may be associated with locally enforced mechanical loading in distinct bone portions, as well as maturation of osteocytes related to bone metabolism discussed above.

Our finding here is consistent with the elevated FGF23 levels in osteocytes in *Dmp1*-deficient mice[26] but not phenotypes in transgenic overexpression of Dmp1 and Dmp1 C-terminal fragment recently reported by Martin *et al*.[52] Neither of transgenic mice carrying full-length Dmp1 nor Dmp1 C-terminal fragment showed significant changes in FGF23 production from the bone and serum. Although changes in serum levels of parathyroid hormone and 1,25-dihydroxyvitamin in these transgenic mice were not investigated, it is probable that the local overdose effect of DMP1 on FGF23 production may be compensated by systemic factors.

The MAPK pathways are ancient signal transducers that regulate a variety of physiological processes, such as cell growth and differentiation, apoptotic cell death and survival.[53,54] Our findings suggest that MAPK signaling is involved in the local regulation of FGF23 in osteocytes, further highlighting the significance of this pathway in bone metabolism.

Materials and Methods

Reagents

Recombinant DMP1, osteopontin (rat) and matrix extracellular phosphoglycoprotein (human and mouse) were from R&D system (Minneapolis, MN, USA). Actin cytoskeleton and focal adhesion staining kits were purchased from Millipore Corporation (Billerica, MA, USA). Collagen and poly L-lysine-coated culture chambers were obtained from IWAKI (Tokyo, Japan). The FGF23 ELISA kit was obtained from KAINOS LABORATORIES, Inc. (Tokyo, Japan). Specific PCR primers for Fgf23, Dmp1 *Runx2*, *Osx*, *Col1a*, *Alp*, *Osc*, *Sost* and *GAPDH* were synthesized by Eurofins, Inc. (Tokyo, Japan). The FAK inhibitor (Focal Adhesion Kinase Inhibitor II) was purchased from Calbiochem (San Diego, CA, USA), the mitogen-activated protein kinase inhibitor (U0126) was purchased from Promega Corporation (Madison, WI, USA), the PI3K inhibitor (LY294002) was purchased from Cell Signaling Technology, Inc. (Beverly, MA, USA) and the ROCK inhibitor (Y-27632) was purchased from Wako (Osaka, Japan). Anti-DMP1 was purchased from Takara (Tokyo, Japan). Rat anti-FGF23 was purchased from R&D Systems. Anti-phospho FAK, anti-FAK, anti-phospho ERK, anti-ERK, anti-phospho-p38 MAPK, anti-p38 MAPK and anti-β-tubulin were purchased from Cell Signaling Technology, Inc. All other chemicals and reagents were of analytical grade.

Animals and preparation of skeletal tissues

Wiser strain male rats 4 and 16 weeks of age were used. All animal experiments were approved by the local ethics committee for animal research (Tokyo Medical and Dental University). After fixation in 4% paraformaldehyde in phosphate-buffered saline at 4 °C for 2–4 weeks and embedding in paraffin, 5-μm serial longitudinal sections were sliced and subjected to immunohistochemistry and immunofluorescence staining. Images of the specimens were acquired using an NISE Elements software program (Nikon, Tokyo, Japan).

Cell culture

UMR-106 cells, a clonal line derived from rat osteosarcoma, were obtained from American Type Culture Collection (Manassas, VA, USA) and cultured in Dulbecco's modified Eagle's high-glucose medium (Invitrogen, Carlsbad, CA, USA). The cells were maintained in continuous culture using weekly passage in α-MEM (Gibco BRL, Grand Island, NY, USA). Fetal bovine serum (10%, vol/vol), penicillin (0.1 U ml^{-1}) and streptomycin (100 μg ml^{-1}) were added to the medium, and the cells were incubated at 37 °C in a humidified atmosphere of 5% CO_2. MC3T3-E1 cells, an osteoblastic and clonal cell line derived from murine osteoblasts, were obtained from RIKEN BRC (RCB1126) and cultured in α-MEM (Gibco BRL) using the same culture conditions described above. To detect the expression of FGF23 in these cells, we performed long-term culture with osteogenic medium over 4 weeks, modified as previously described.[47] After 4 weeks of culture in the culture dish, the cells were seeded onto well plates for each assay.

Immunohistochemistry and immunofluorescence

Specimens of the rat femur tissues were fixed in 4% paraformaldehyde and embedded in paraffin wax. Five-micrometer sections were then cut from the paraffin blocks for the immunohistochemical analysis. For antigen retrieval, the sections of rat femur were treated with trypsin digestion for immunostaining of FGF23 and DMP1 and then blocked with 1% bovine serum albumin at room temperature for 30 min. The primary antibodies were added and incubated with rat anti-FGF23 (1:100) and rabbit anti-DMP1 (1:100) at 4 °C overnight. Alexa Fluor 488- or Alexa Fluor 568-conjugated secondary antibodies (Invitrogen) were used for immunofluorescence, respectively. An immunoglobulin-negative control was used to rule out nonspecific binding. For the immunocytochemistry analysis, UMR-106 cells were seeded onto eight-well chambers and allowed to reach ~50% confluence in basal medium. The cells were serum deprived for 24 h and then treated with 100 ng ml^{-1} rDMP1 for 24 h. The cells were then rinsed twice with phosphate-buffered saline and fixed in 4% paraformaldehyde for 10 min. All subsequent steps were determined using rat anti-FGF23, actin cytoskeleton and focal adhesion staining kits (Millipore Corporation) according to the manufacturer's protocol. Wide-field fluorescence images were acquired by a differential interference contrast microscopy, Nikon ECLIPSE Ti (Nikon), and image processing was conducted using NISE elements (Nikon).

Determination of FGF23 production and its gene expression

For the analysis of the release of FGF23 into the medium and *fgf23* gene expression, the cells were seeded on 24-well plates at 1×10^5 cells per well and cultured under serum-deprived conditions for 24 h before being treated with rDMP1. The conditioned medium was collected from the cells after 24 h, and the immunoreactive FGF23 levels were determined using an ELISA assay kit, according to the manufacturer's protocol. The cells on the plate were collected in order to extract total RNA for the analysis of *fgf23* gene expression.

Quantitative real-time PCR

Total cellular RNA was extracted from the cells using the RNeasy Mini Kit (Qiagen, Hilden, Germany) according to the manufacturer's protocol. First-strand cDNA was synthesized from total RNA using oligo(dT) primers and subjected to real-time PCR with LightCycler DNA master SYBR green I (Roche, Mannheim, Germany) using the following specific PCR primers (shown in Supplementary Table 1). The SYBR green signal was detected using a LightCycler Nano system quantitative PCR

machine (Roche). To discriminate specific from nonspecific cDNA products, a melting curve was obtained at the end of each run.

Western blot analysis

The cells were lysed with RIPA buffer (20 mM Tris-HCl, pH 7.5, 150 mM NaCl, 1 mM EDTA, 50 mM β-glycerophosphate, 1% NP-40, 1 mM Na_3VO_4, 1 × phosphatase inhibitor cocktail and 1 × protease inhibitor cocktail), and the protein concentration was determined using a BCA Protein Assay with bovine serum albumin as the standard. A total of 40 μg of protein was denatured in SDS sample buffer and resolved on 10% SDS-polyacrylamide gel. The proteins were transferred in 25 mM Tris, 192 mM glycine and 20% methanol to polyvinylidene difluoride membranes. The blots were blocked with Tris-buffered saline (20 mM Tris-HCl (pH 7.5) and 137 mM NaCl) plus 0.1% Tween 20 containing 5% bovine serum albumin. After blocking, the membrane was allowed to react with the specific antibodies, and the detection of specific proteins was carried out using enhanced chemiluminescence according to the manufacturer's instructions. Loading differences were normalized using β-tubulin antibodies.

Confocal three-dimensional imaging

Confocal optical sectioning was performed using a LSM5 Pascal5 confocal laser scanning microscope (Carl Zeiss, Oberkochen, Germany) with PlanFluor objectives (× 20, numerical aperture = 0.8, or × 63, numerical aperture = 1.4). Two laser lines, 488 and 543 nm, were used. The z-series of the optical images was obtained with a 0.5-μm or a 0.29-μm step size four times and then subjected to Kalman averaging.

Three-dimensional reconstruction and fluorescence morphometry *in silico*

The three-dimensional fluorescence images of the FGF23 and DMP1 immunofluorescence intensities and the degree of focal adhesion formation on immunocytochemistry were evaluated from a z-series of confocal laser scanning images using the IMARIS software program (Bitplane, Zürich, Switzerland).[33,34] All parameters were measured using the Surface function of IMARIS by rotating the three-dimensional-reconstructed images as previously described. The relative intensity of each signal spot to that of the highest intensity in each scanned specimen was calculated and statistically analyzed.

Statistical analysis

The data are expressed as the mean ± s.d. Statistical differences were determined in PSS for Mac (SPSS, Munich, Germany). When groups were compared, the one-way analysis of variance was followed by Duncan's *post hoc* multiple comparison analysis. *, $^{\#}P < 0.05$.

Conflict of Interest

The authors declare no conflict of interest.

Acknowledgements

We express sincere gratitude to the laboratory members of Professor Takeshi Imamura in Ehime University and Dr Yoshihiro Tamamura in Tokyo Medical and Dental University for their helpful comments on this work. The current work was supported by a Grant-in-Aid for Scientific Research from the Japan Society for the Promotion of Science (JSPS) to TI and AY, and a Grant-in-Aid for Scientific Research on Innovative Areas "Fluorescence Live Imaging" (No. 22113002) of the Ministry of Education, Culture, Sports, Science, and Technology (MEXT) MEXT to TI.

References

1. Bonewald LF. The amazing osteocyte. *J Bone Miner Res* 2011;**26**:229–238.
2. Bonewald LF, Johnson ML. Osteocytes, mechanosensing and Wnt signaling. *Bone* 2008;**42**:606–615.
3. Bonewald LF, Wacker MJ. FGF23 production by osteocytes. *Pediatr Nephrol* 2013;**28**: 563–568.
4. Xiong J, Onal M, Jilka RL, Weinstein RS, Manolagas SC, O'Brien CA. Matrix-embedded cells control osteoclast formation. *Nat Med* 2011;**17**:1235–1241.
5. Tatsumi S, Ishii K, Amizuka N, Li M, Kobayashi T, Kohno K *et al.* Targeted ablation of osteocytes induces osteoporosis with defective mechanotransduction. *Cell Metab* 2007;**5**:464–475.
6. Nakashima T, Hayashi M, Fukunaga T, Kurata K, Oh-Hora M, Feng JQ *et al.* Evidence for osteocyte regulation of bone homeostasis through RANKL expression. *Nat Med* 2011;**17**:1231–1234.
7. Lin C, Jiang X, Dai Z, Guo X, Weng T, Wang J *et al.* Sclerostin mediates bone response to mechanical unloading through antagonizing Wnt/beta-catenin signaling. *J Bone Miner Res* 2009;**24**:1651–1661.
8. Cowin SC, Moss-Salentijn L, Moss ML. Candidates for the mechanosensory system in bone. *J Biomech Eng* 1991;**113**:191–197.
9. Burger EH, Klein-Nulend J. Mechanotransduction in bone--role of the lacuno-canalicular network. *FASEB J* 1999;**13**(Suppl):S101–S112.
10. Fukumoto S. The role of bone in phosphate metabolism. *Mol Cell Endocrinol* 2009;**310**:63–70.
11. Fukumoto S, Martin TJ. Bone as an endocrine organ. *Trends Endocrinol Metab* 2009;**20**: 230–236.
12. Yamashita T, Yoshioka M, Itoh N. Identification of a novel fibroblast growth factor, FGF-23, preferentially expressed in the ventrolateral thalamic nucleus of the brain. *Biochem Biophys Res Commun* 2000;**277**:494–498.
13. Weber TJ, Liu S, Indridason OS, Quarles LD. Serum FGF23 levels in normal and disordered phosphorus homeostasis. *J Bone Miner Res* 2003;**18**:1227–1234.
14. Shimada T, Mizutani S, Muto T, Yoneya T, Hino R, Takeda S *et al.* Cloning and characterization of FGF23 as a causative factor of tumor-induced osteomalacia. *Proc Natl Acad Sci USA* 2001;**98**:6500–6505.
15. Liu S, Guo R, Simpson LG, Xiao ZS, Burnham CE, Quarles LD. Regulation of fibroblastic growth factor 23 expression but not degradation by PHEX. *J Biol Chem* 2003;**278**: 37419–37426.
16. Sitara D, Razzaque MS, Hesse M, Yoganathan S, Taguchi T, Erben RG *et al.* Homozygous ablation of fibroblast growth factor-23 results in hyperphosphatemia and impaired skeletogenesis, and reverses hypophosphatemia in Phex-deficient mice. *Matrix Biol* 2004; **23**:421–432.
17. Liu S, Zhou J, Tang W, Jiang X, Rowe DW, Quarles LD. Pathogenic role of Fgf23 in Hyp mice. *Am J Physiol Endocrinol Metab* 2006;**291**:E38–E49.
18. Ubaidus S, Li M, Sultana S, de Freitas PH, Oda K, Maeda T *et al.* FGF23 is mainly synthesized by osteocytes in the regularly distributed osteocytic lacunar canalicular system established after physiological bone remodeling. *J Electron Microsc (Tokyo)* 2009;**58**:381–392.
19. Berndt T, Kumar R. Phosphatonins and the regulation of phosphate homeostasis. *Annu Rev Physiol* 2007;**69**:341–359.
20. Gattineni J, Bates C, Twombley K, Dwarakanath V, Robinson ML, Goetz R *et al.* FGF23 decreases renal NaPi-2a and NaPi-2c expression and induces hypophosphatemia in vivo predominantly via FGF receptor 1. *Am J Physiol Renal Physiol* 2009;**297**: F282–F291.
21. Shimada T, Hasegawa H, Yamazaki Y, Muto T, Hino R, Takeuchi Y *et al.* FGF-23 is a potent regulator of vitamin D metabolism and phosphate homeostasis. *J Bone Miner Res* 2004;**19**:429–435.
22. Gattineni J, Twombley K, Goetz R, Mohammadi M, Baum M. Regulation of serum 1,25(OH)2 vitamin D3 levels by fibroblast growth factor 23 is mediated by FGF receptors 3 and 4. *Am J Physiol Renal Physiol* 2011;**301**:F371–F377.
23. Ben-Dov IZ, Galitzer H, Lavi-Moshayoff V, Goetz R, Kuro-o M, Mohammadi M *et al.* The parathyroid is a target organ for FGF23 in rats. *J Clin Invest* 2007;**117**: 4003–4008.
24. Lavi-Moshayoff V, Wasserman G, Meir T, Silver J, Naveh-Many T. PTH increases FGF23 gene expression and mediates the high-FGF23 levels of experimental kidney failure: a bone parathyroid feedback loop. *Am J Physiol Renal Physiol* 2010;**299**:F882–F889.
25. Canalejo R, Canalejo A, Martinez-Moreno JM, Rodriguez-Ortiz ME, Estepa JC, Mendoza FJ *et al.* FGF23 fails to inhibit uremic parathyroid glands. *J Am Soc Nephrol* 2010;**21**:1125–1135.
26. Feng JQ, Ward LM, Liu S, Lu Y, Xie Y, Yuan B *et al.* Loss of DMP1 causes rickets and osteomalacia and identifies a role for osteocytes in mineral metabolism. *Nat Genet* 2006;**38**:1310–1315.

27. Toyosawa S, Shintani S, Fujiwara T, Ooshima T, Sato A, Ijuhin N *et al.* Dentin matrix protein 1 is predominantly expressed in chicken and rat osteocytes but not in osteoblasts. *J Bone Miner Res* 2001;**16**:2017–2026.
28. Thompson DL, Sabbagh Y, Tenenhouse HS, Roche PC, Drezner MK, Salisbury JL *et al.* Ontogeny of Phex/PHEX protein expression in mouse embryo and subcellular localization in osteoblasts. *J Bone Miner Res* 2002;**17**:311–320.
29. MacDougall M, Gu TT, Luan X, Simmons D, Chen J. Identification of a novel isoform of mouse dentin matrix protein 1: spatial expression in mineralized tissues. *J Bone Miner Res* 1998;**13**:422–431.
30. George A, Sabsay B, Simonian PA, Veis A. Characterization of a novel dentin matrix acidic phosphoprotein. Implications for induction of biomineralization. *J Biol Chem* 1993;**268**:12624–12630.
31. Ducy P, Zhang R, Geoffroy V, Ridall AL, Karsenty G. Osf2/Cbfa1: a transcriptional activator of osteoblast differentiation. *Cell* 1997;**89**:747–754.
32. D'Souza RN, Cavender A, Sunavala G, Alvarez J, Ohshima T, Kulkarni AB *et al.* Gene expression patterns of murine dentin matrix protein 1 (Dmp1) and dentin sialophosphoprotein (DSPP) suggest distinct developmental functions in vivo. *J Bone Miner Res* 1997;**12**: 2040–2049.
33. Makino Y, Takahashi Y, Tanabe R, Tamamura Y, Watanabe T, Haraikawa M *et al.* Spatiotemporal disorder in the axial skeleton development of the Mesp2-null mouse: a model of spondylocostal dysostosis and spondylothoracic dysostosis. *Bone* 2013;**53**: 248–258.
34. Watanabe T, Tamamura Y, Hoshino A, Makino Y, Kamioka H, Amagasa T *et al.* Increasing participation of sclerostin in postnatal bone development, revealed by three-dimensional immunofluorescence morphometry. *Bone* 2012;**51**:447–458.
35. Himeno-Ando A, Izumi Y, Yamaguchi A, Iimura T. Structural differences in the osteocyte network between the calvaria and long bone revealed by three-dimensional fluorescence morphometry, possibly reflecting distinct mechano-adaptations and sensitivities. *Biochem Biophys Res Commun* 2012;**417**:765–770.
36. Forrest SM, Ng KW, Findlay DM, Michelangeli VP, Livesey SA, Partridge NC *et al.* Characterization of an osteoblast-like clonal cell line which responds to both parathyroid hormone and calcitonin. *Calcif Tissue Int* 1985;**37**:51–56.
37. Gray TK, Flynn TC, Gray KM, Nabell LM. 17 beta-estradiol acts directly on the clonal osteoblastic cell line UMR106. *Proc Natl Acad Sci USA* 1987;**84**:6267–6271.
38. Martin TJ, Ingleton PM, Coulton LA, Melick RA. Metabolic properties of hormonally responsive osteogenic sarcoma cells. *Clin Orthop Relat Res* 1979;**140**:247–254.
39. Partridge NC, Alcorn D, Michelangeli VP, Kemp BE, Ryan GB, Martin TJ. Functional properties of hormonally responsive cultured normal and malignant rat osteoblastic cells. *Endocrinology* 1981;**108**:213–219.
40. Carrillo-Lopez N, Roman-Garcia P, Rodriguez-Rebollar A, Fernandez-Martin JL, Naves-Diaz M, Cannata-Andia JB. Indirect regulation of PTH by estrogens may require FGF23. *J Am Soc Nephrol* 2009;**20**:2009–2017.
41. Samadfam R, Richard C, Nguyen-Yamamoto L, Bolivar I, Goltzman D. Bone formation regulates circulating concentrations of fibroblast growth factor 23. *Endocrinology* 2009;**150**:4835–4845.
42. Kolek OI, Hines ER, Jones MD, LeSueur LK, Lipko MA, Kiela PR *et al.* 1alpha,25-Dihydroxyvitamin D3 upregulates FGF23 gene expression in bone: the final link in a renal-gastrointestinal-skeletal axis that controls phosphate transport. *Am J Physiol Gastrointest Liver Physiol* 2005;**289**:G1036–G1042.
43. Farrow EG, Yu X, Summers LJ, Davis SI, Fleet JC, Allen MR *et al.* Iron deficiency drives an autosomal dominant hypophosphatemic rickets (ADHR) phenotype in fibroblast growth factor-23 (Fgf23) knock-in mice. *Proc Natl Acad Sci USA* 2011;**108**:E1146–E1155.
44. von Marschall Z, Fisher LW. Dentin matrix protein-1 isoforms promote differential cell attachment and migration. *J Biol Chem* 2008;**283**:32730–32740.
45. Wu H, Teng PN, Jayaraman T, Onishi S, Li J, Bannon L *et al.* Dentin matrix protein 1 (DMP1) signals via cell surface integrin. *J Biol Chem* 2011;**286**:29462–29469.
46. Hynes RO. Integrins: bidirectional, allosteric signaling machines. *Cell* 2002;**110**:673–687.
47. Wang X, Wang S, Li C, Gao T, Liu Y, Rangiani A *et al.* Inactivation of a novel FGF23 regulator, FAM20C, leads to hypophosphatemic rickets in mice. *PLoS Genet* 2012;**8**:e1002708.
48. Quarles LD. Endocrine functions of bone in mineral metabolism regulation. *J Clin Invest* 2008;**118**:3820–3828.
49. Narayanan K, Ramachandran A, Hao J, He G, Park KW, Cho M *et al.* Dual functional roles of dentin matrix protein 1. Implications in biomineralization and gene transcription by activation of intracellular Ca2+ store. *J Biol Chem* 2003;**278**:17500–17508.
50. Kamioka H, Sugawara Y, Murshid SA, Ishihara Y, Honjo T, Takano-Yamamoto T. Fluid shear stress induces less calcium response in a single primary osteocyte than in a single osteoblast: implication of different focal adhesion formation. *J Bone Miner Res* 2006;**21**: 1012–1021.
51. Sugawara Y, Kamioka H, Ishihara Y, Fujisawa N, Kawanabe N, Yamashiro T. The early mouse 3D osteocyte network in the presence and absence of mechanical loading. *Bone* 2013;**52**: 189–196.
52. Martin A, David V, Li H, Dai B, Feng JQ, Quarles LD. Overexpression of the DMP1 C-terminal fragment stimulates FGF23 and exacerbates the hypophosphatemic rickets phenotype in Hyp mice. *Mol Endocrinol* 2012;**26**:1883–1895.
53. Junttila MR, Li SP, Westermarck J. Phosphatase-mediated crosstalk between MAPK signaling pathways in the regulation of cell survival. *FASEB J* 2008;**22**:954–965.
54. Greenblatt MB, Shim JH, Glimcher LH. Mitogen-activated protein kinase pathways in osteoblasts. *Annu Rev Cell Dev Biol* 2013;**29**:63–79.

Supplementary Information accompanies the paper on the BoneKEy website (http://www.nature.com/bonekey).